place the ssDNA-binding mouth of DnaG distal from DnaB, orienting the active site of primase inward, toward the center of the ring, where it is positioned to accept ssDNA as it is extruded from DnaB (Fig. 4, right). Alternatively, it is possible that mechanistic differences between 6:6 and 6:1 helicase-primase systems lead to different relative orientations of the primase active sites. The true relative locations of these domains awaits high-resolution study of the primase-helicase complexes in *E. coli* and phage T7.

References and Notes

1. D. Brutlag, R. Schekman, A. Kornberg, *Proc. Natl. Acad. Sci. U.S.A.* **68**, 2826 (1971).
2. A. Kornberg and T. A. Baker, *DNA Replication* (Freeman, New York, ed. 2, 1992).
3. E. L. Zechner, C. A. Wu, K. J. Marians, *J. Biol. Chem.* **267**, 4054 (1992).
4. K. Tougu and K. J. Marians, *J. Biol. Chem.* **271**, 21398 (1996).
5. Y. B. Lu, P. V. Ratnakar, B. K. Mohanty, D. Bastia, *Proc. Natl. Acad. Sci. U.S.A.* **93**, 12902 (1996).
6. A. Yuzhakov, Z. Kelman, M. O'Donnell, *Cell* **96**, 153 (1999).
7. T. Kitani, K. Yoda, T. Ogawa, T. Okazaki, *J. Mol. Biol.* **184**, 45 (1985).
8. K. J. Marians, *Annu. Rev. Biochem.* **61**, 673 (1992).
9. K. Tougu, H. Peng, K. J. Marians, *J. Biol. Chem.* **269**, 4675 (1994).
10. W. Sun, J. Tormo, T. A. Steitz, G. N. Godson, *Proc. Natl. Acad. Sci. U.S.A.* **91**, 11462 (1994).
11. J. L. Keck, D. D. Roche, A. S. Lynch, J. M. Berger, data not shown.
12. T5-overexpression plasmids encoding residues 111 to 433 of *E. coli* DnaG (DnaG-RNAP) preceded by a hexahistidine tag were constructed and overexpressed in SG13009/pREP4 cells. Cells were lysed by sonication and the extract was clarified by centrifugation. Soluble DnaG-RNAP was purified by applying the lysate to a nickel-affinity column and eluting the protein with 200 mM imidazole. His-tagged DnaG-RNAP was further purified by size-exclusion chromatography and concentrated to >10 mg ml^{-1}. Selenomethionine-incorporated protein was expressed as described [G. D. Van Duyne, R. F. Standaert, A. P. Karplus, S. L. Schreiber, J. Clardy, *J. Mol. Biol.* **229**, 105 (1993)] and was purified as per the unsubstituted protein, except that 2 mM dithiothreitol was included in all purification buffers. Concentrated His-tagged DnaG-RNAP was dialyzed against 10 mM Hepes (pH 7.5), 100 mM NaCl, and diluted to a final concentration of ~10 mg ml^{-1} before crystallization. Crystals of His-tagged DnaG-RNAP were formed by hanging drop vapor diffusion by mixing 1 μl of protein with 1 μl of well solution [18 to 21% polyethylene glycol (PEG) 4000, 5% PEG200, 30% ethylene glycol, 0.2 M ammonium acetate, 0.05 M sodium acetate (pH 5.0), 0.1% dioxane, 2 to 8 mM $SrCl_2$, YCl_2, or $DyCl_3$] and equilibrating the drop against 1 ml of well solution at room temperature for several days. Two nonisomorphous crystal forms were observed, depending on the divalent metal that was used; with YCl_2 or $DyCl_3$, small platelike crystals (~200 μm by 100 μm by 10 μm) of symmetry $P2_12_12_1$ with unit cell lengths $a = 38$, $b = 56$, $c = 140$ Å were formed; with $SrCl_2$, thicker bar-shaped crystals (~200 μm by 75 μm by 75 μm) of symmetry $P2_12_12_1$ with unit cell lengths $a = 39$, $b = 58$, $c = 149$ Å were formed.
13. Selenomethionine-incorporated $SrCl_2$-based crystals were solved by MAD phasing to 2.5 Å. Data were indexed and scaled with MOSFLM [A. G. W. Leslie, *Newsletter on Protein Crystallography No. 26* (Science and Engineering Research Council, Daresbury Laboratory, Warrington, UK, 1992)] and SCALA [W. Kabash, *J. Appl. Crystallogr.* **21**, 916 (1988)]. Selenium sites were determined with SOLVE [T. C. Terwilliger and J. Berendzen, *Acta Crystallogr. D* **52**, 749 (1996)] and refined with MLPHARE [Z. Otwinowski, *Proc. CCP4 Study Weekend* (Science and Engineering Research Council, Daresbury Laboratory, Warrington, UK, 1991), p. 80]. Solvent-flattening with DM [K. Cowtan, *Joint CCP4 ESF-EACBM Newlett. Protein Crystallogr.* **31**, 34 (1994)] yielded readily interpretable electron-density maps for model building (Fig. 1B) with O [T. A. Jones, J. Y. Zou, S. W. Cowan, M. Kjeldgaard, *Acta Crystallogr. A* **47**, 110 (1991)]. Elves, an automated structure solution package, was used throughout data analysis and map construction (J. Holton and T. Alber, in preparation). The initial model was refined against a high-resolution native data set to 1.6 Å resolution with an R_{work} of 23.1% and an R_{free} of 27.6% by using Refmac/ARP [G. N. Murshudov, A. A. Vagin, E. J. Dodson, *Acta Crystallogr. D* **53**, 240 (1997); V. S. Lamzin and K. S. Wilson, *Acta Crystallogr. D* **49**, 129 (1993)]. The final model includes residues 115 to 428, with the exception of residues 192 to 194 and 287, for which electron density was not observed. No bond angles for this model fall into either disallowed or generously allowed regions of Ramachandrian space.
14. The structure of the YCl_2-based crystal form was solved by molecular replacement with AMORE [J. Navaza, *Acta Crystallogr. D* **50**, 1507 (1994)] and the refined $SrCl_2$ structure as an initial model. The molecular replacement solution was refined to 1.7 Å resolution with an R_{work} of 20.9% and a R_{free} of 26.3% by using Refmac/ARP [G. N. Murshudov, A. A. Vagin, E. J. Dodson, *Acta Crystallogr. D* **53**, 240 (1997); V. S. Lamzin and K. S. Wilson, *Acta Crystallogr. D* **49**, 129 (1993)]. Four Y^{2+} ions were modeled, three of which bound in the putative active site of DnaG-RNAP. The occupancies of these metals were estimated by using $F_o - F_c$ difference maps until the density for these sites was appropriately accounted for. The final model included residues from 115 to 427, excluding residues 192 to 194, for which electron density was not observed. The rmsd for all common C_α atoms between the two structures is 0.6 Å. No bond angles for this model fall into either disallowed or generously allowed regions of Ramachandrian space.
15. L. Holm and C. Sander, *J. Mol. Biol.* **233**, 123 (1993).
16. L. Aravind, D. D. Leipe, E. V. Koonin, *Nucleic Acids Res.* **26**, 4205 (1998).
17. J. M. Berger, D. Fass, J. C. Wang, S. C. Harrison, *Proc. Natl. Acad. Sci. U.S.A.* **95**, 7876 (1998).
18. J. Versalovic and J. R. Lupski, *Gene* **136**, 281 (1993).
19. T. V. Ilyina, A. E. Gorbalenya, E. V. Koonin, *J. Mol. Evol.* **34**, 351 (1992).
20. G. Ziegelin, N. A. Linderoth, R. Calendar, E. Lanka, *J. Bacteriol.* **177**, 4333 (1995).
21. W. Sun, J. Schoneich, G. N. Godson, *J. Bacteriol.* **181**, 3761 (1999).
22. M. D. Nichols, K. DeAngelis, J. L. Keck, J. M. Berger, *EMBO J.* **18**, 6177 (1999).
23. T. A. Steitz, *J. Biol. Chem.* **274**, 17395 (1999).
24. H. H. Egelman, X. Yu, R. Wild, M. M. Hingorani, S. S. Patel, *Proc. Natl. Acad. Sci. U.S.A.* **92**, 3869 (1995).
25. X. Yu, M. M. Hingorani, S. S. Patel, E. H. Egelman, *Nature Struct. Biol.* **3**, 740 (1996).
26. T. Kusakabe, K. Baradaran, J. Lee, C. C. Richardson, *EMBO J.* **17**, 1542 (1998).
27. M. Carson, *J. Appl. Crystallogr.* **24**, 958 (1991).
28. J. D. Thompson, T. J. Gibson, F. Plewniak, F. Jeanmougin, D. G. Higgins, *Nucleic Acids Res.* **25**, 4876 (1997).
29. S. A. Benner, M. A. Cohen, G. H. Gonnet, *Protein Eng.* **7**, 1323 (1994).
30. W. Kabsch and C. Sanders, *Biopolymers* **22**, 2577 (1983).
31. A. Nicholls, K. A. Sharp, B. Honig, *Proteins* **11**, 281 (1991).
32. D. L. Ollis, P. Brick, R. Hamlin, N. G. Xuong, T. A. Steitz, *Nature* **313**, 762 (1985).
33. M. J. Jezewska, S. Rajendran, D. Bujalowska, W. Bujalowski, *J. Biol. Chem.* **273**, 10515 (1998).

34. We thank the 5.0.2 beamline staff at the Advanced Light Source (Lawrence Berkeley National Laboratories) for assistance with measurements and J. Holton and O. Littlefield for helpful discussions. We also thank M. Botchan, R. Calendar, N. Cozzarelli, S. Gradia, R. Fennell-Fezzie, and K. DeAngelis for assistance with the manuscript and E. Egelman for providing electron micrograph reconstructions of the T7 primase-helicase. Supported by the G. Harold and Leila Y. Mathers Charitable Foundation (J.M.B.) and The Jane Coffin Childs Memorial Fund for Medical Research (J.L.K.). The crystallographic coordinates of both structures have been deposited in the RCSB Protein Data Bank (accession codes: 1DD9 and 1DDE).

6 December 1999; accepted 9 February 2000

Mitotic Misregulation and Human Aging

Danith H. Ly,[1] David J. Lockhart,[2] Richard A. Lerner,[1]* Peter G. Schultz[1,2]*

Messenger RNA levels were measured in actively dividing fibroblasts isolated from young, middle-age, and old-age humans and humans with progeria, a rare genetic disorder characterized by accelerated aging. Genes whose expression is associated with age-related phenotypes and diseases were identified. The data also suggest that an underlying mechanism of the aging process involves increasing errors in the mitotic machinery of dividing cells in the postreproductive stage of life. We propose that this dysfunction leads to chromosomal pathologies that result in misregulation of genes involved in the aging process.

The question of why we age has intrigued mankind since the beginning of time. Extensive studies of model systems including yeast, *Caenorhabditis elegans*, *Drosophila*, and mice as well as studies of human progerias and cellular senescence have identified a number of processes thought to contribute to the aging phenotype (*1*). These include the effects of oxidative damage associated with cellular metabolism and genome instabilities such as telomere shortening, mitochondrial mutations, and chromosomal pathologies. To gain greater insights into the mechanisms that control life-span and age-related phenotypes, we have studied gene

[1]Department of Chemistry and the Skaggs Institute for Chemical Biology, The Scripps Research Institute, 10550 North Torrey Pines Road, La Jolla, CA 92037, USA. [2]Genomics Institute of the Novartis Research Foundation, 3115 Merryfield Row, San Diego, CA 92121, USA.

*To whom correspondence should be addressed.

regulation of normal and premature aging in actively dividing cells. Studies of fibroblasts derived from young, middle-age, and old-age humans and from humans with Hutchinson-Gilford progeria revealed sets of genes that correlate with, and hence likely contribute to, age-related phenotypes and diseases. The results also suggest that mitotic errors in dividing cells may lead to the altered expression of this collection of genes.

Ten closely matched dermal fibroblast cell lines were classified into four categories based on their chronological and diagnostic similarities: normal young (NY), normal middle (NM), normal old (NO), and Hutchinson-Gilford progeria (P) (*2*). Collectively, NY, NM, and NO samples allow examination of the expression levels of various genes throughout the natural aging process. Hutchinson-Gilford progeria, on the other hand, is a rare genetic disease in which those affected display at a very early age features typically associated with natural old age, including loss of or graying of hair, diminished subcutaneous fat, cardiovascular disease, and skeletal abnormalities (*3*). Actively dividing early passage fibroblasts from each age group were initially examined by phase contrast and fluorescence microscopy to characterize age-related morphological changes (*2*). For each group, the elliptical morphology characteristic of fibroblast nuclei was observed in the majority of cells. However, in contrast to fibroblasts from NY and NM individuals, whose nuclei appeared normal, the NO and P groups had a significant proportion of cells exhibiting aberrant nuclear morphology including multilobed nuclei and irregular nuclear boundaries. The NO and P populations also had a higher proportion of cells with multiple nuclei, consistent with reports of age-dependent increases in micronucleation in human lymphocytes (*4*). Flow-activated cell sorting (FACS) analysis of the same fibroblasts from the NY and NM groups revealed very similar populations of cells with 2N, S, and 4N DNA content. However, NO and P fibroblasts showed higher percentages of 4N DNA content (Fig. 1), consistent with the larger number of binucleated cells observed by microscopy.

To examine the transcriptional profiles (mRNA abundance) of these fibroblasts, asynchronous and actively dividing cells were cultured in vitro to about 60% confluency (*2*, *5*). Messenger RNA levels were analyzed with high-density oligonucleotide arrays containing probes for more than 6000 known human genes. Expression patterns for each age group (NM, NO, and P) were compared with NY fibroblasts (baseline). Only those changes that were reproducible across all comparisons and all independent replicates were considered further (Fig. 2). On the basis of these conservative criteria, we found that 61 genes (~1% of the genes monitored) showed consistent expression level changes more than twofold between young and middle age. More than half of these 61 genes can be grouped into two functional classes, (i) genes whose products are involved in cell cycle progression (25%) (Table 1) and (ii) genes involved in maintenance and remodeling of the extracellular matrix (ECM) (31%) (Table 2). The first group of genes are all involved in mitosis and are down-regulated between 2.6- and 12.5-fold. These include cyclins A, B, and F, which are typically up-regulated at the G_2-M cell cycle phase transition and control mitotic progression (*6*); polo kinase (pLK), which regulates both spindle assembly and cyclin-dependent kinase 1–cyclin B (Cdk1-cyclin B) activation (*7*, *8*); and p55CDC, which participates in the mitotic checkpoint (*9*). In addition, a group of proteins involved in spindle assembly and chromosome segregation are down-regulated, including the centromere-associated proteins CENP-A (*10*), mitosin (CENP-F) (*11*), and histone H2A.X (*12*), as well as the kinesin-related proteins, mitotic centromere-associated kinesin (MCAK) (*13*), mitotic kinesin-like protein-1 (*14*), and kinesin-like spindle protein (HKSP) (*15*). Transcription factors associated with the G_2-M transition, including B-myb (*16*, *17*) and hepatocyte nuclear factor–3/fork head homolog (HFH-11A) (*18*), are also down-regulated. Myb is known to

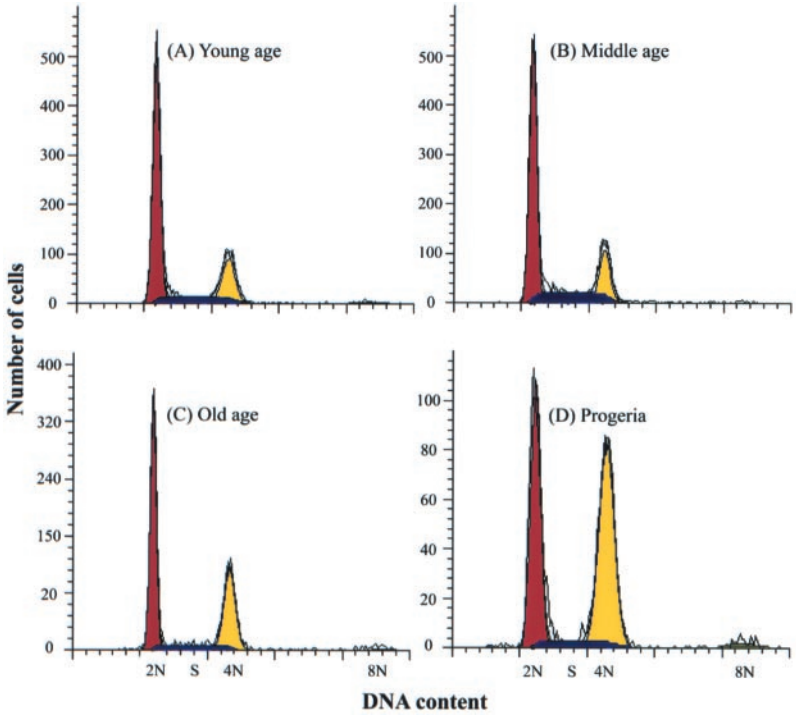

Fig. 1. Actively dividing cells were grown in culture to about 60% confluency before they were ethanol-fixed and stained with propidium iodide for DNA content. The gated histograms were generated and curve-fitted with ModFit LT (Verity Software House, Topsham, ME). (**A**) NY (CRL7469): 2N, 62%; S, 14%; 4N, 24%. (**B**) NM (CRL7581): 2N, 60%; S, 19%; 4N, 21%. (**C**) NO (AG04059B): 2N, 52%; S, 11%; 4N, 37%. (**D**) P (AG06297B): 2N, 40%; S, 8%; 4N, 52%. The cell cycle parameters for these cell lines are representative of each age group with 3% SD in NY, NM, and NO, and 6% SD in progeria. Colors indicate specific DNA content: red, 2N; blue, S; yellow, 4N; light yellow, 8N.

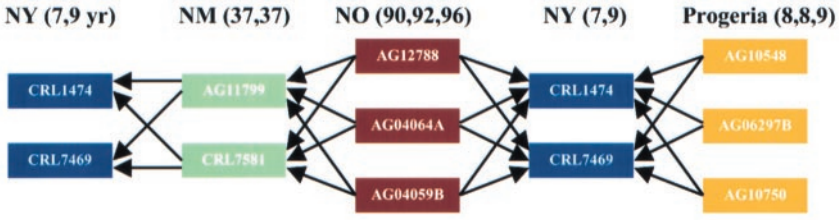

Fig. 2. A comparative analysis of gene expression in natural and accelerated human aging. Expression profiles from cells from middle- and old-age participants and participants with progeria were compared with cells from young participants. The selection criteria were set conservatively such that the selected genes were required to have the same pattern of expression (all up-regulated or all down-regulated) with a twofold change of transcriptional levels or greater in all comparisons.

Table 1. A comparison of changes in gene expression in middle age, old age, and progeria versus young. The magnitude of the changes reported was computed as the average values over the set of comparisons, where the highest and lowest values were excluded. Colors indicate genes that are common across age groups. Red, genes common across all three age groups; brown, genes common in middle and old age; blue, genes common in old age and progeria; black, genes unique to an age group.

Middle Age

Cell Cycle Control Proteins

Acc.#	FoldΔ	Gene Name
X13293	-4.8	B-myb
U74612	-3.3	Hepatocyte nuclear factor-3/fork head homolog 11A (HFH-11A)
Z36714	-12.5	Cyclin F
X51688	-5.4	Cyclin A
M25753	-2.9	Cyclin B
U01038	-2.8	pLK
U05340	-2.9	p55CDC

Chromosomal Processing and Assembly

U30872	-2.6	Mitosin (CENP-F)
X67155	-3.5	Mitotic kinesin-like protein-1
U37426	-3.6	Kinesin-like spindle protein (HKSP)
X14850	-2.2	Histone (H2A.X)
U14518	-3.3	Centromere protein-A (CENP-A)
U63743	-2.8	Mitotic centromere-associated kinesin
X13546	-2.0	Non-histone chromosomal protein HMG-17

Protein Processing

U73379	-2.3	Cyclin-selective ubiquitin carrier protein

Old Age

Cell Cycle Control Proteins

Acc.#	FoldΔ	Gene Name
X13293	-4.9	B-myb
U74612	-9.0	Hepatocyte nuclear factor-3/fork head homolog 11A (HFH-11A)
Z36714	-13.1	Cyclin F
X51688	-5.8	Cyclin A
M25753	-5.2	Cyclin B
U01038	-3.0	pLK
U05340	-4.3	p55CDC
S78187	-7.6	CDC25B
U56816	-8.7	Kinase Myt1 (Myt1)
X54941	-2.6	Ckshs1 Cks1 protein homologue
M30448	-2.2	Casein kinase II beta subunit
U37022	-4.0	Cyclin-dependent kinase 4 (CDK4)
U49844	-3.0	FRAP-related protein (ATR, ATM)
X74008	-3.0	Protein phosphatase 1 gamma

Chromosomal Processing and Assembly

U30872	-2.6	Mitosin (CENP-F)
X67155	-3.5	Mitotic kinesin-like protein-1
U37426	-3.6	Kinesin-like spindle protein (HKSP)
X14850	-2.2	Histone (H2A.X)
U14518	-3.3	Centromere protein-A (CENP-A)
U63743	-2.8	Mitotic centromere-associated kinesin
X13546	-2.0	Non-histone chromosomal protein HMG-17
M97856	-3.0	Histone binding protein
D38076	-2.9	RanBP1 (Ran-binding protein 1)
X62534	-4.3	HMG-2
Y08612	-4.1	Nup88 protein
L43631	-2.5	Scaffold attachment factor (SAF-B)
U33286	-3.6	Chromosomal segregation gene homolog CAS
D26361	-4.3	KIAA0042 (Centromere protein-E)
M37583	-3.0	Histone (H2A.Z)
U72342	-2.3	Platelet activating factor acetylhydrolase (45 Kda subunit LIS1)
D43948	-2.6	KIA00097 (36% similar to yeast Suppressor of tubulin STU2)

Protein Processing

U73379	-3.5	Cyclin-selective ubiquitin carrier protein
AB003102	-2.7	26S proteasome subunit p44.5
AB003103	-3.7	Proteasome subunit p55
D00760	-2.6	Proteasome subunit HC3
D00762	-3.2	Proteasome subunit HC8
D11094	-3.2	MSS1 (26S proteasome subunit)
D78275	-2.4	Proteasome subunit p42

Progeria

Cell Cycle Control Proteins

Acc.#	FoldΔ	Gene Name
X13293	-7.0	B-myb
U74612	-8.7	Hepatocyte nuclear factor-3/fork head homolog 11A (HFH-11A)
Z36714	-8.7	Cyclin F
S78187	-3.4	CDC25B
U56816	-11.3	Kinase Myt1 (Myt1)
X54941	-4.5	Ckshs1 Cks1 protein homologue
M30448	-2.0	Casein kinase II beta subunit
L08246	-2.2	Myeloid cell differentiation protein (MCL1)

Chromosomal Processing and Assembly

X14850	-6.1	Histone H2A.X
U14518	-4.3	Centromere protein-A (CENP-A)
U63743	-4.8	Mitotic centromere-associated kinesin
X13546	-3.0	Non-histone chromosomal protein HMG 17
M97856	-2.9	Histone binding protein
D38076	-2.7	RanBP1 (Ran-binding protein 1)
X62534	-4.4	HMG-2
Y08612	-3.5	Nup88 protein
L43631	-3.2	Scaffold attachment factor (SAF-B)
U35451	-2.5	Heterochromatin proten p25

regulate cellular proliferation and differentiation, and HFH-11A is a homolog of *daf*-16, a protein that has been shown to regulate key metabolic and developmental genes and plays a role in regulating life-span in *C. elegans* (*17*).

A significant number of genes involved in remodeling of the ECM also show altered expression. For example, human macrophage metalloproteinase (HME) and stromelysin 2 are increased 24- and 14-fold, respectively, whereas the protease inhibitors urokinase inhibitor (PAI-2) and cystatin M increase five- to ninefold. A number of proteoglycan cell adhesion proteins are also up-regulated, including dermatopontin, fibromodulin, and thrombospondin, as well as collagens VI and XV and cartilage oligomeric matrix protein (COMP). The preponderance of differentially expressed mitotic and ECM genes compared with genes involved in other cellular processes likely reflects some level of coordinated regulation between these classes of genes (*19*). The remainder of genes whose expression levels differ consistently by twofold or more include key enzymes involved in the conversion of arachidonic acids to the prostaglandins and thromboxane, such as prostaglandin endoperoxidase synthase 2, endoperoxide synthase type II, cyclooxygenase 2, and endoperoxidase synthase (5- to 30-fold changes). Increasing levels of these enzymes with age may affect a large number of systemic physiological processes, including platelet aggregation, muscle and kidney function, bone formation, and various inflammatory processes.

Analysis of gene expression in fibroblasts isolated from old versus young individuals again revealed a down-regulation of genes involved in the G_2-M phase of the cell cycle (Table 1). Some of these same cell cycle genes that were down-regulated in middle age versus young cells are more significantly down-regulated in old-age individuals. In addition, other cell cycle genes are affected. For example, the cell cycle proteins FRAP-related protein [FRP1, a homolog of ataxia-telangiectasia mutated (ATM) and its related protein (ATR)], CKS1, and Myt1 are down-regulated three- to ninefold; all are involved in the G_2-M DNA dependent checkpoint pathway, which ensures fidelity before entry into mitosis (*20*). CDC25B, a key protein triggering entry into mitosis, is also down-regulated. Expression of some of these genes may be controlled by common cell cycle transcriptional control elements (*21*). There is also an increase in the number of down-regulated genes involved in spindle assembly and segregation, including CENP-E, HMG-2, Ran BP1 (also involved in nuclear transport and regulation of polyadenylation), and scaffold attachment factor. DNA synthesis and repair genes {e.g., thymidylate synthase, minichromosome maintenance protein, Rad 2, poly(adenosine diphosphate–ribose) [poly-(ADP-ribose)] synthetase, and proliferating cell nuclear antigen} and RNA synthesis and processing genes (RNA helicases) are also down-regulated. The importance of the down-regulation of some of these repair genes has been clearly demonstrated. For example, in the case of poly(ADP-ribose) synthetase (also known as a polymerase, or PARP), partial inhibition by antisense agents or complete removal by gene knockout results in increased DNA strand breaks, recombination, gene amplification, and aneuploidy (*22*). Decreased expression levels are also found for proteasomal proteins, which are a core component of the anaphase-promoting complex (APC) and are responsible for the timing of the metaphase to anaphase transition (the final stage of cell division) and other key events in the cell cycle (Table 1). A significant number of genes whose products affect the ECM are again differentially expressed in fibroblasts from old-age individuals; however, the expression levels are less pronounced when compared with that of NM and NY fibroblasts. Genes involved in arachidonic acid oxidation continue to be affected, as do genes involved in lipid transport and metabolism.

Other changes in gene expression occur in old age that are not seen in middle age. For example, genes involved in the stress response and heat shock proteins are up-regulated, including αβ-crystallin, which is thought to be involved in maintenance of the cellular cytoskeleton (*23*), and a heat shock serine protease human HtrA, which is overexpressed in osteoarthritic cartilage. Mitochondrial genes are down-regulated, which is consistent with age-related mitochondrial dysfunction (*1*). Similar changes in a number of stress-response and metabolic genes were observed in expression profiles of aged versus young skeletal muscle from mouse (*24*). Transcript levels of genes involved in oncogenesis, signal transduction, and the cellular immune response also change and may be linked with age-related diseases.

A comparison of mRNA transcript profiles between progeria and normal young cells reveals a consistent and significant change in the expression of 76 genes. Many of these genes overlap with those found in the comparison of young and old-age samples (Tables 1 and 2). In particular, genes involved in cell division and DNA or RNA synthesis and processing are commonly down-regulated in NO and P. ECM-related genes continue to represent a significant fraction of those genes whose expression levels change. Particularly in progeria, one observes changes in expression of the caldesmons, which are actin-binding proteins involved in cell cycle–dependent reorganization of the cytoskeleton (*25*); desmoplakin I, which plays a role in intracellular adhesive junctions (*26*); and autotaxins, which are extracellular phosphodiesterases involved in cellular chemotaxis. Transforming growth factor–β (TGF-β) expression also increases 12-fold, consistent with changes in expression of the large number of genes that affect the ECM (*27*). Genes involved in fatty acid transport and oxidation also vary in similar ways, as with old age and progeria.

Comparison of the genes whose transcript levels change as a function of natural and premature aging reveals classes of genes that can be linked to aging-related phenotypes and diseases. For example, osteoblast (OB)-specific factor 2 (osteoprotegerin) (*28*) and OB-cadherin (*29*) play key roles as transcriptional activator and adhesion molecules in bone formation, respectively. Their down-regulation in old age may be linked to bone diseases such as osteoporosis. HME (*30*) is up-regulated with age and has been shown to be associated with joint destruction in rheumatoid arthritis. Down-regulation of the hyaluronic acid (HA) synthase may also contribute to joint disease; depletion of HA is observed in early experimental osteoarthritis in dogs (*31*). Cartilage oligomeric matrix protein is significantly up-regulated in old age and has been shown to correlate with disease activity in rheumatoid arthritis and is also arthritogenic when expressed in rat cartilage (*32*). Cathepsin C, an oligomeric lysosomal protease whose loss of function results in periodontal disease and palmoplantar keratosis, is down-regulated 10-fold in old age (*33*). In general, the altered expression of a large number of genes that influence the ECM may contribute to age-related changes in the derma.

Expression of other genes possibly linked to age-related diseases is also observed. The breast cancer susceptibility protein–1 (BRCA-1) associated Ring domain protein (BARD1), which binds the NH_2-terminus of BRCA-1, a protein implicated in DNA repair and cell cycle checkpoint regulation, is down-regulated in old-age and progeria cells (*34*). Down-regulation of BARD1 may deleteriously affect BRCA-1 function and may be linked with age-related sporadic breast cancer; mutations of BARD1 have been identified in breast, ovarian, and uterine cancers (*35*). The hFRP-1 gene, which is also down-regulated in old age, is a homolog of the gene *ATM* mutated in ataxia-telangiecstasia (A-T). A-T is an autosomal recessive disorder characterized by progressive neurodegeneration, immune deficiencies, premature aging, chromosomal instability, and radiation sensitivity (*36*). ATM, like BRCA-1, plays a key role in the cellular response to DNA breaks, including activation of cell cycle checkpoints and DNA repair. Down-regulation of genes involved in these pathways would result in an increase in genetic instability and sensitivity to reactive oxygen species. αβ-crystallin expression increases with old age (*37*). It is also overexpressed in a number of neurolog-

Table 2. A comparison of changes in gene expression in middle age, old age, and progeria versus young. Methods and colors are as in Table 1.

Middle Age

Acc.#	FoldΔ	Gene Name
Fatty Acids Synthesis		
D28235	-5.3	Prostaglandin endorperoxidase synthase-2
L15326	-7.1	Endoperoxide synthase type II
U04636	-29.7	Cyclooxygenase-2 (hCox-2)
M59979	11.6	Prostaglandin endoperoxidase synthase
Extracellular Matrix (ECM)/Cytoskeleton		
U05291	9.7	Fibromudulin
D87258	2.6	Cancellous bone osteoblast serine protease
M31551	8.5	Urokinase inhibitor (PAI-2)
L23808	23.5	Metalloproteinase (HME)
L32137	7.6	Germline oligomeric matrix protein (COMP)
U62800	5.3	Cystatin M (CST6)
L10035	3.3	Crystallin beta-B2
L12350	4.4	Thrombospondin
Z22865	5.8	Dermatopontin
U94332	4.9	Osteoprotegrin
X07820	13.5	Metalloproteinase stromelysin-2
HG4480-HT4833	7.7	Collagen, type VI, alpha 2
L25286	4.3	Collagen, type XV, alpha1
Growth Factors		
Y00787	5.0	MDNCF

Old Age

Acc.#	FoldΔ	Gene Name
DNA /RNA Synthesis and Repair		
HG4074-HT4344	-5.7	Rad2
D00596	-5.8	Thymidylate synthase
D21063	-10.0	Minichromosome maintenance protein
U90426	-4.6	Nuclear RNA helicase
U63743	-6.4	DEAD box RNA helicase-like protein
J03473	-3.6	Poly(ADP-ribose) synthetase
J05614	-5.7	Proliferating cell nuclear antigen (PCNA)
Fatty Acids Synthesis		
D28235	-3.0	Prostaglandin endorperoxidase synthase-2
L15326	-3.1	Endoperoxidase synthase type II
U04636	-7.1	Cyclooxygenase-2 (hCox-2)
M59979	8.0	Prostaglandin endoperoxidase synthase
D50840	-4.6	Ceramide glucosyltransferase
U73514	-10.7	Short-chain alcohol dehydrogenase (XH98G2)
Extracellular Matrix (ECM)/Cytoskeleton		
U05291	8.2	Fibromodulin
D87258	3.0	Cancellous bone osteoblast serine protease
M31551	-3.0	Urokinase Inhibitor (PAI-2)
L23808	5.7	Metalloproteinase (HME)
L32137	15.4	Germline oligomeric matrix protein (COMP)
U62800	21.0	Cystatin M (CST6)
S45630	2.9	Alpha B-crystallin=Rosenthal fiber component
U03272	-4.5	Fibrillin-2
D13666	-7.2	Osteoblast specific factor 2 (OSF-2os)
U54804	-9.5	HAS2 (hyaluronan synthase)
D21255	-3.4	OB-cadherin-2
U50939	-2.6	Amyloid precursor protein-binding protein 1 (APP-BP1)
X87212	-5.9	Cathepsin C
Growth Factors		
Y00787	-4.1	MDNCF
D50683	-2.8	TGF-beta IIR alpha
Tumor Suppressors		
U76638	-4.5	BRCA1-associated RING domain (BARD1)

Progeria

Acc.#	FoldΔ	Gene Name
DNA/RNA Synthesis and Repair		
HG4074-HT4344	-5.8	Rad2
D00596	-5.1	Thymidylate synthase
D21063	-7.4	Minichromosome maintenance protein
U90426	-2.5	Nuclear RNA helicase
U63743	-4.8	DEAD box RNA helicase-like protein
J03473	-2.8	Poly(ADP-ribose) synthetase
Fatty Acids Synthesis		
D28235	-4.1	Prostaglandin endoperoxidase synthase-2
L15326	-4.1	Endoperoxidase synthase type II
U04636	-11.8	Cyclooxygenase-2 (hCox-2)
D50840	-2.5	Ceramide glucosyltransferase
Extracellular Matrix (ECM)/Cytoskeleton		
U05291	4.9	Fibromodulin
D87258	2.3	Cancellous bone osteoblast serine protease
M31551	-4.7	Urokinase Inhibitor (PAI-2)
HG174-HT174	5.9	Desmoplakin 1
HG2743-HT2845	3.3	Caldesmon 1, Alt. splice3, non-muscle
HG2743-HT2846	3.4	Caldesmon 1, Alt. splice4, non-muscle
M83216	5.7	Aorta caldesmon
HG2743-HT3926	5.1	Caldesmon 1, alt splice 6,Non-muscle
X05232	-29.5	Stromelysin
U54804	-6.5	HAS2 (hyaluronan synthase)
Growth Factors		
Y00787	-4.1	MDNCF
AB000584	11.6	TGF-beta superfamily protein
Tumor Suppressors		
U76638	-3.5	BRCA1-associated RING domain protein (BARD1)
Protein Synthesis/processing		
L35594	-14.8	Autotaxin
L46720	-12.0	Autotaxin-t (atx-t)

ical disorders such as Alzheimer's disease, Diffuse Lewy Body disease, and Alexander's disease, suggesting a possible link between this protein and age-related neurologic disease. αβ-Crystallin has also been implicated in the formation of age-related nuclear cataracts (*38*). The amyloid precursor protein (APP)–binding protein, which binds at the COOH-terminal of APP, the proteolysis site in the generation of β amyloid peptides, is down-regulated with age (*39*). TGF-β, a key growth factor that regulates tissue homeostasis and whose sustained expression is responsible for tissue fibrosis, is highly up-regulated in progeria, consistent with the biopsies from the progeria patients. COX-2 expression is down-regulated in NM, NO, and P samples. COX-2 knockout mice exhibit abnormalities in the kidney, heart, and ovaries that result in renal dysplasia, cardiac fibrosis, cancer, gastric insufficiency, and female infertility—all of which are related to aging (*40*). Thus, analysis of gene expression across a larger collection of human genes and in a number of different tissues specifically affected by these and other age-related diseases may allow the identification of key genes associated with diseases of aging, which may provide potential points for therapeutic intervention. Clearly, it will be of interest to carry out similar studies with cell types associated with specific diseases such as breast epithelial cells.

In addition to identifying genes that contribute to the aging phenotype, the analysis of gene expression in natural aging and progeria may also provide insights into the underlying mechanisms of the aging process. A comparison of cells from middle- and old-age humans reveals a common set of genes with altered expression levels. These genes are principally involved in the G_2-M phase of the cell cycle and in remodeling the ECM; they are likely linked through changes in the cellular cytoskeleton that occur during cell division. A comparison of gene expression in old age and progeria also reveals disregulation of many of the same genes, as well as additional genes involved in DNA or RNA synthesis and processing. The large number of mitosis-related genes that are down-regulated in middle-age, old-age, and progeria fibroblasts does not simply reflect altered cell cycle populations resulting from differential growth rates. This is supported by the fact that the G_0-G_1 and G_2-M populations in young and middle age are virtually identical and that the cells also grow at the same rate. In old-age and progeria cells, the 4N DNA content is even higher, reflecting either a larger number of cells in G_2-M or an increased incidence of tetraploidy. The genes whose expression is altered in middle-age, old-age, and progeria also do not correspond with those observed in cellular senescence (*41*). Indeed, a recent re-examination of fibroblast culture replicative life-span does not show a correlation with donor age (*42*). In addition, the transcript profiles described here do not resemble those of quiescent (*19*), contact-inhibited (*43*), or G_1-arrested cell populations (*44*), nor do the changes in gene expression observed here correspond to those observed in the aged hypothalamus (*43*) or skeletal muscle (*24*). In the latter case, a marked stress response was observed along with a lower expression of metabolic and biosynthesis genes. Although a number of the same changes were observed here, the majority of changes we observe in cell cycle, ECM, fatty acid oxidation, and disease-related genes were not observed in muscle or hypothalamus. The altered expression of these genes observed at middle age and elaborated in old age and progeria are likely specific to mitotic versus postmitotic cells.

We suggest that an altered expression of genes involved in cell division occurs with age. These changes result in increased rates of somatic mutation, leading to numerical and structural chromosome aberrations and mutations that manifest themselves as an aging phenotype. Previous studies have demonstrated an increase in aneuploidy with increased age (*45*), and down-regulation of mitotic genes has been shown to lead to aneuploidy in experimental models. For example, both a motorless mitotic centromere-associated kinesin (MCAK) and antisense inhibition of MCAK lead to chromosome lagging during anaphase (*13*). It has also been argued that mutations in presenilin 1 and 2, which are associated with both the interphase kinetochore and centrosome and account for most early onset familial Alzheimer's disease, may result in chromosome pathologies (*46*). Aneuploidy associated with chromosome 21 is involved in Down syndrome, a disease characterized by some features of premature aging. Misregulation of genes involved in cell division may be the result of an intrinsic lack of fidelity that arises in the absence of selection in the postreproductive stage. Alternatively, the growing loss of fidelity may result from the cumulative effects of oxidative damage associated with metabolism, which are slowed by caloric restriction (*24*). In fact, there may be multiple entry points into this process. For example, Werner syndrome, which is characterized by the premature appearance of aging in young adults (*47*), shows an increased rate of chromosomal abnormalities caused by mutations in a DNA helicase or exonuclease enzyme known as WRN.

Chromosome pathologies that begin to occur in dividing cells relatively early in life (postreproductive stage) may then lead to misregulation of key structural, signaling, and metabolic genes associated with the aging phenotype, such as osteoporosis, Alzheimer's disease, arthritis, and so forth. Misregulation of this sort is expected to increase in each round of cell division. It may be propagated to other normal mitotic (e.g., leukocytes, epithelial cells, glial cells, and so forth) and postmitotic (e.g., neurons, muscles, and so forth) cells through changes in the ECM and oxidized fatty acid derivatives that affect signaling pathways. Aging, therefore, may occur gradually and in mosaic patterns, rather than as a uniform phenomenon as in cancerous growth, which is clonal. Additional studies are required before we can understand the aging process in complex organisms, both in mitotic and postmitotic tissue, but the studies reported here highlight important mechanisms that may contribute to aging and age-related problems.

References and Notes

1. F. B. Johnson, D. A. Sinclair, L. Guarente, *Cell* **96**, 291 (1999).
2. These cell lines were initiated from primary explants taken antemortem from separate individuals, and the patients are described as follows: *age*, year:month; *sex*, male (M), female (F); *race*, caucasian (C); *PDL*, population doubling (number of times cells divided to double the population); *phenotype*, P, NO, NY, or NM. Cell lines AG10548 (8:4, M, C, 5, P), AG10750 (9:4, M, C, 6, P), AG06297B (8:2, M, C, 33, P), AG12788 (90:00, M, C, 9, O), AG04064A (92:00, M, C, 15, O), AG04059B (96:00, M, C, 11, O), and AG11799 (37:00, M, C, 19, NM) were obtained from the Coriell Institute for Medical Research (Camden, NJ). Cell lines CRL-1474 (7:00, M, C, 25, NY), CRL-7469 (9:00, M, C, 22, NY), and CRL-7581 (37:00, M, C, 20, NM) were obtained from the American Type Culture Collection (Manassas, VA). Tables of data are available at *Science* Online at www.sciencemag.org/feature/data/1046164.shl. Cells were cultured (minimum essential medium Eagle–Earle balanced salt solution containing 2× concentrations of vitamins, essential and nonessential amino acids, and 10% fetal bovine serum) in 5% CO_2 at 37°C and were split in a 1:2 ratio at confluency with trypsin-EDTA. Bromodeoxyuridine (BrdU) incorporation was performed according to Becton Dickinson (Franklin Lakes, NJ) protocols and imaged with epifluorescence microscopy. After a 48-hour incubation with 10 μM BrdU and staining with antibody to BrdU–fluorescein isothiocyanate (FITC), more than 90% of the fibroblasts derived from old-age and progeria individuals showed intense staining of the nucleus, a similar ratio compared with cells from young and middle-age individuals. The analysis was based on 200 cells counted.
3. T. W. Brown, *Am. J. Clin. Nutr.* **55**, 1222S (1992).
4. J. Nath, J. D. Tucker, J. C. Hando, *Chromosoma* **103**, 725 (1995).
5. Cells were grown under identical conditions for three additional doublings to about 60% confluency. Polyadenylated RNAs were isolated and converted to cDNA, followed by in vitro transcription cRNA synthesis. The biotinylated cRNAs were then hybridized to the HuGeneFL oligonucleotide arrays (Affymetrix, Santa Clara, CA), which contain probes for more than 6000 known human genes. All procedures were performed according to prescribed Affymetrix protocols.
6. J. Yang and S. Kornbluth, *Trends Cell. Biol.* **9**, 207 (1999).
7. E. A. Nigg, *Curr. Opin. Cell. Biol.* **10**, 776 (1998).
8. D. M. Glover, H. Ohkura, A. Tavares, *J. Cell Biol.* **135**, 1681 (1996).
9. M. Kallio, J. Weinstein, J. R. Daum, D. J. Burke, G. J. Gorbsky, *J. Cell Biol.* **141**, 1393 (1998).
10. R. D. Shelby, O. Vafa, K. F. Sullivan, *J. Cell Biol.* **136**, 501 (1997).
11. G. K. T. Chan, B. T. Schaar, T. J. Yen, *J. Cell Biol.* **143**, 49 (1998).
12. Y. Watabe *et al.*, *J. Biol. Chem.* **271**, 25126 (1996).
13. T. Maney, A. W. Hunter, M. Wagenbach, L. Wordeman, *J. Cell Biol.* **142**, 787 (1998).
14. C. Nislow, V. A. Lombillo, J. R. McIntosh, *Nature* **359**, 543 (1992).
15. C. E. Walczak and T. J. Mitchison, *Cell* **85**, 943 (1996).

16. A. Sala *et al.*, *Proc. Natl. Acad. Sci. U.S.A.* **94**, 532 (1997).
17. I. H. Oh and E. P. Reddy, *Oncogene* **18**, 3017 (1999).
18. D. E. Clevidence *et al.*, *Proc. Natl. Acad. Sci. U.S.A.* **90**, 3948 (1993).
19. L. Svensson *et al.*, *J. Biol. Chem.* **274**, 9636 (1999); V. R. Iyer *et al. Science* **283**, 83 (1999).
20. B. Furnari, N. Rhind, P. Russell, *Science* **277**, 1495 (1997).
21. J. Zwicker and R. Muller, *Trends Genet.* **13**, 3 (1997).
22. C. M. Simbulan *et al.*, *Proc. Natl. Acad. Sci. U.S.A.* **96**, 13191 (1999).
23. F. A. van de Klundert, M. L. Gijsen, P. R. van den Ijssel, L. H. Snoeckx, W. W. de Jong, *Eur. J. Cell. Biol.* **75**, 38 (1998).
24. C.-K. Lee, R. G. Klopp, R. Weindruch, T. A. Prolla, *Science* **285**, 1390 (1999).
25. R. Ishikawa, S. Yamashiro, K. Kohama, F. Matsumura, *J. Biol. Chem.* **273**, 26991 (1998).
26. G. I. Gallicano *et al.*, *J. Cell. Biol.* **143**, 2009 (1998).
27. J. Massague, *Annu. Rev. Biochem.* **67**, 753 (1998).
28. P. Ducy *et al.*, *Cell* **89**, 747 (1997).
29. M. Okazaki *et al.*, *J. Biol. Chem.* **269**, 12092 (1994).
30. Y. Ichikawa, C. Yamada, T. Horiki, Y. Soshina, M. Uchiyama, *Clin. Exp. Rheumatol.* **16**, 533 (1998).
31. K. Kawasaki, M. Ochi, Y. Uchio, N. Adachi, M. Matsusaki, *J. Cell. Physiol.* **179**, 142 (1999).
32. S. Carlsen, A. S. Hanson, H. Olsson, D. Heinegard, R. Holmdahl, *Clin. Exp. Immunol.* **114**, 477 (1998).
33. C. Toomes *et al.*, *Nature Genet.* **23**, 421 (1999).
34. Y. Jin *et al.*, *Proc. Natl. Acad. Sci. U.S.A.* **94**, 12075 (1997).
35. T. H. Hao Thai *et al.*, *Hum. Mol. Genet.* **7**, 195 (1998).
36. C. Barlow *et al.*, *Cell* **86**, 159 (1996).
37. M. P. Bova *et al.*, *Proc. Natl. Acad. Sci. U.S.A.* **96**, 6137 (1999).
38. R. J. Truscott, Y. C. Chen, D. C. Shaw, *Int. J. Biol. Macromol.* **22**, 1 (1998).
39. S. Tomita, Y. Korino, T. Suzuki, *J. Biol. Chem.* **273**, 19304 (1998).
40. M. Oshima *et al.*, *Cell* **87**, 803 (1996).
41. J. R. Smith and O. M. Pereira-Smith, *Science* **273**, 63 (1996).
42. V. J. Cristofalo, R. G. Allen, R. J. Pignolo, B. G. Martin, J. C. Beck, *Proc. Natl. Acad. Sci. U.S.A.* **95**, 10614 (1998).
43. D. H. Ly, D. J. Lockhart, R. A. Lerner, P. G. Schultz, data not shown.
44. R. Cho *et al.*, *Mol. Cell* **2**, 65 (1998).
45. P. A. Jacobs, M. Brunton, W. M. C. Brown, R. Doll, H. Goldstein, *Nature* **197**, 1080 (1963).
46. J. Li, M. Xu, H. Zhou, J. Ma, H. Potter, *Cell* **90**, 917 (1997).
47. K. Hanada *et al.*, *Proc. Natl. Acad. Sci. U.S.A.* **94**, 3860 (1997).
48. We thank the Skaggs Institute for Chemical Sciences and the American Chemical Society Irving Sigal Postdoctoral Fellowship (D.L.) for financial support, D. Wemmer and G. Rosania for helpful discussions, A. Su for computational support, K. Sullivan for assistance with microscopy, and J. Trotter for help with flow cytometry.

12 October 1999; accepted 8 February 2000

Similar Requirements of a Plant Symbiont and a Mammalian Pathogen for Prolonged Intracellular Survival

K. LeVier,[1] R. W. Phillips,[2] V. K. Grippe,[2] R. M. Roop II,[2] G. C. Walker[1]*

***Brucella abortus*, a mammalian pathogen, and *Rhizobium meliloti*, a phylogenetically related plant symbiont, establish chronic infections in their respective hosts. Here a highly conserved *B. abortus* homolog of the *R. meliloti bacA* gene, which encodes a putative cytoplasmic membrane transport protein required for symbiosis, was identified. An isogenic *B. abortus bacA* mutant exhibited decreased survival in macrophages and greatly accelerated clearance from experimentally infected mice compared to the virulent parental strain. Thus, the *bacA* gene product is critical for the maintenance of two very diverse host-bacterial relationships.**

Rhizobia establish agriculturally important symbioses with leguminous plants (*1*), whereas brucellae are highly infectious pathogens of animals and cause the human disease brucellosis (*2*, *3*). Despite leading to exceedingly different outcomes in interactions with their respective eukaryotic hosts, the in-host life-styles of these closely phylogenetically related bacteria (*4*) show striking parallels. In the establishment of chronic infection, both rhizobia and brucellae are endocytosed by host cells, where they then undergo adaptive changes and ultimately live for prolonged periods in intracellular, acidic, host-membrane–bound compartments (*1–3*, *5*, *6*).

Rhizobium meliloti bacA mutants invade alfalfa nodules like wild-type bacteria, but lyse upon release into plant cells before they can differentiate and establish a chronic host infection (*7*). BacA is predicted to be a cytoplasmic membrane transport protein with seven transmembrane domains (*7*, *8*). BacA is 64% identical to, and functionally interchangeable with, the *Escherichia coli* SbmA protein inferred to be a transporter of bleomycin and microcins B17 and J25 (*9*). *R. meliloti bacA* mutants also have increased resistance to bleomycin (*9*).

We identified a *B. abortus* DNA fragment that included a monocistronic 1248-nucleotide open reading frame (ORF) (GenBank AF244996) (*10*) that encodes a predicted protein of 47.3 kD with 68.2% identity to *R. meliloti* BacA. In both *B. abortus* and *R. meliloti*, *bacA* is flanked by an upstream gene for a putative transporter and a downstream gene, transcribed in the opposite direction, that has similarity to a putative bacterial secreted protein. We constructed an allele (*bacA1*) of the *bacA* gene in which 41% of the *bacA* ORF was replaced with a drug resistance cassette (strain KL7) (*11*). As with *R. meliloti*, disruption of *bacA* function resulted in increased resistance to bleomycin (Fig. 1) (*12*).

The capacity of the brucellae to survive and replicate in host macrophages is critical to their ability to produce disease (*2*). The *bacA1* mutant and its wild-type parent were opsonized and used to infect cultured murine macrophages (*13*). During the first 24 hours post infection (p.i.), both strains showed net intracellular killing by the phagocytes (Fig. 2). The virulent wild-type strain showed characteristic net replication in macrophages at 36 hours p.i. and beyond, but the *bacA1* mutant did not appear to recover after the initial period of killing.

To determine if this defect in intracellular replication in macrophages correlated with an inability to establish a chronic infection in the host, we experimentally infected BALB/c mice with the *bacA1* mutant and its wild-type parent (*14*). BALB/c mice represent the classic model for chronic *B. abortus* infection in the host (*15*): Substantial numbers of brucellae can be recovered from the spleens and livers of mice infected with virulent strains

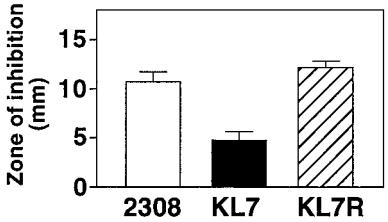

Fig. 1. Increased resistance of the *B. abortus bacA* mutant to killing by bleomycin. Strains 2308 (wild-type), KL7 (Δ*bacA*), and KL7R (reconstructed Δ*bacA*) were spread onto Schaedler agar plates and overlayed with filter paper disks containing bleomycin. The diameter of cleared zones of *B. abortus* growth inhibition in response to the drug was measured after 72 hours. Data are presented as the mean ± SD (n = 5).

[1]Department of Biology, Massachusetts Institute of Technology, Cambridge, MA 02139, USA. [2]Department of Microbiology and Immunology, Louisiana State University Health Sciences Center, Shreveport, LA 71130, USA.

*To whom correspondence should be addressed. E-mail: gwalker@mit.edu